PHYSICAL REVIEW E **72**, 1 (2005)

Mode locking the cell cycle

Frederick R. Cross*
The Rockefeller University, 1230 York Avenue, New York, New York, 10021, USA

Eric D. Siggia†
Center for Studies in Physics and Biology, The Rockefeller University, 1230 York Avenue, New York, New York 10021, USA
(Received 4 April 2005)

A characteristic property of nonlinear oscillatory systems is their ability to mode lock to a periodic, external, driving signal. In an $n:m$ mode-locked state, the driven system executes n oscillations to every m oscillations of the driving signal, with a constant phase relationship between the two oscillations. We investigate mode locking for a mathematical model of the cell cycle in budding yeast. We determine which variables are most effective in coupling an external stimulus to the cell cycle oscillator, and speculate about whether experiments are feasible and informative for this model organism.

DOI: XXXX PACS number(s): 87.17.−d, 05.45.−a, 82.40.Bj

INTRODUCTION

Mutations that lead to visible aberrations in the cell cycle of budding yeast were isolated over 30 years ago, and the gradual elucidation of the function of the affected gene and their biochemical properties have made this system one of the best understood genetic regulatory networks in biology [1,2]. Homologues to all the key genes in budding and fission yeast exist in metazoans and make the cell cycle oscillator truly universal. This oscillator is not a simple two variable affair in analogy to its physical counterpart, and even with the limited markers that could be scored 30 years ago, dozens of genes were found that affected the process. This is in part because of the complex reconfigurations the cell has to undergo to divide, and the number of genes that are coordinately regulated is about 15% of the total [3]. This is not an anomaly but typical of the reprogramming that a cell undergoes during mating, sporulation, starvation, etc. It is fitting that some of the first mathematical models of biological networks in eukaryotic cells were for the cell cycle [4–7]

To model such a system by differential equations in analogy with a well mixed chemical reaction (perhaps allowing for a few separate subcellular compartments) is a daunting task, since few of the kinetic constants are easy to determine. There is no in vitro reconstitution of the yeast cell cycle, unlike the simpler system in frog egg extracts [2]. In fact most of the available data for modeling is still genetic, where one or more components of the system are removed, and the functioning of others observed, often qualitatively. The strength of genetics is that processes can be ordered in a pathway (e.g., B is downstream of A if mutating A and B is equivalent to mutating B alone) without knowing all the intermediates. Thus A activates B can become A represses C represses B when a new component C is discovered, without vitiating the earlier description involving A and B alone. However, pathways are seldom strictly serial and mutations that produce an easily observed phenotype often have complex ramifications throughout the cell that we are unable to characterize. The resulting cells can be severely impaired.

Mathematicians long ago posed the question of how to obtain insight into the solutions of the differential equations describing physical systems without having to integrate them [8]. One outcome was a theory based on geometric reasoning that enumerated "typical" behaviors of nonlinear systems when the solution bifurcated from one type of solution to another. Bifurcation theory has recently been applied to the differential equation model for the cell cycle in Ref. 9.

Another application of geometric reasoning was the observation that a subset of the cell cycle genes acts as a relaxation oscillator [4] with two locally stable states that are destabilized by a slowly varying parameter (the mass in the yeast model). The metastability and hysteresis inherent in a relaxation oscillator has been observed in egg extracts [10,11] and yeast [12]. A unification of the negative feedback oscillator that drives the rapidly cycling egg extracts, with the system in budding yeast, was recently formulated by Cross [13]. A completely different way to tame the parameter explosion concomitant with a differential equation model is to resort to a binary on/off description for the genes or their activities [14].

In this paper we propose in analogy to the observation of hysteresis another consequence of the geometric description of an oscillating system, namely that it should mode lock to an external periodic perturbation. We illustrate the effect with a version of Chen *et al.*'s cell cycle model [6], though clearly the interest is to achieve this in the laboratory. Experiments of the type we propose can be done on wild type cells and hence the appeal of learning something about the natural system (wt) without taking it apart.

RESULTS

To understand the essence of mode locking, consider a stable periodic orbit in a system with many variables. Stabil-

*FAX: 212-327-7193.
Electronic address: fcross@mail.rockefeller.edu
†FAX: 212-327-8544.
Electronic address: siggiae@mail.rockefeller.edu

ity means that nearby orbits are attracted onto the periodic one. With some technical assumptions, the phase variable on the periodic orbit serves as a coordinate for all points nearby, if one associates with them, the phase to which they converge as they approach the orbit. By assumption, the phase along the periodic orbit is always increasing with time (no stagnation points), so that we can choose an angular coordinate ϕ to make the angular velocity a constant, ω. Finally, we idealize the external perturbation as a series of instantaneous impulses with period T. Each impulse has a magnitude characterized by a "force," f, in the physical variables describing the system. Then the dynamics for small f can be characterized as

$$d\phi/dt = \omega + g(\phi) f \Delta(t), \tag{1}$$

where $g(\phi)$ is a periodic function of ϕ (magnitude of order 1) obtained by projecting from the physical variable to the phase variable, and $\Delta(t)$ is a sum of unit impulses (Dirac delta functions) spaced by the period T. (If the motion remains close to the periodic orbit, then it can be described by ϕ and thus the function g only depends on ϕ.)

Let ϕ_0 be the phase just before a pulse, then the phase ϕ_1 just before the next pulse is

$$\phi_1 = \phi_0 + g(\phi_0) f + \omega T \pmod{2\pi}. \tag{2}$$

To understand the long term evolution of Eq. (1) it suffices to characterize the behavior of the so-called Poincaré map Eq. (2). Mode locking means that the system's period equals a rational multiple (n/m) of the period of the external perturbation for a range of periods T. In terms of Eq. (2), this requires that after m (integer) iterations of Eq. (2), ϕ arguments by $2\pi n$ and returns precisely to its initial value on the circle. In the simplest case (1:1) when the system period locks to the external one, a fixed point ϕ^* of Eq. (2) is defined by

$$g(\phi^*) f + \omega T = 2\pi. \tag{3}$$

Thus locking occurs for T within an interval of size f around the natural period, $2\pi\omega$. Locking also implies there is a fixed phase, ϕ^*, between the perturbation and the solution whose value adjusts to accommodate the value of T.

Figure 1 shows graphically for Eq. (2) how a pair of stable-unstable fixed points appears as ωT is varied for fixed f. In terms of Eq. (3), for smooth functions g, there is a pair of roots near the extrema, with one positive and one negative derivative.

Linearizing Eq. (2) around $\phi^*(\delta\phi = \phi - \phi^*)$ gives

$$\delta\phi_1 = [1 + f g'(\phi^*)] \delta\phi_0. \tag{4}$$

Thus the fixed point with negative derivative is stable, as should be obvious already from Fig. 1. Perturbations decay to zero, exponentially in time, but do so slowly since f is assumed to be small. It should be plausible that the external perturbation does not have to be an impulse; what matters is the phase shift it produces during one traversal of the periodic orbit. Also, the sign of f is immaterial. Flipping it merely interchanges the stable and unstable fixed points.

Budding yeast divide asymmetrically [Fig. 2(a)]. The daughter is smaller than the mother and undergoes a longer

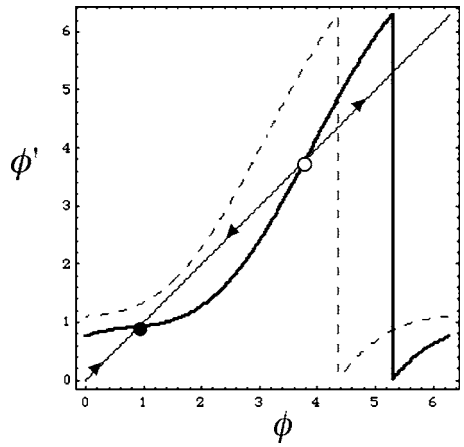

FIG. 1. The Poincaré map, Eq. (2), is a function that maps the circle (ϕ from 0 to 2π) onto itself and is invertible. The solid curve shows a value of ωT that intersects the diagonal line in two points giving rise to stable (closed circle) and unstable (open circle) fixed points [Eq. (4)]. The dashed curve shows a larger value of ωT (ϕ_1 moves upward) with no fixed points. Fixed points occur when $(\omega T - 2\pi)$ is of order the size "bump" in the curve, i.e., $\sim f$. The arrows show the flow of successive iterates of the map, into the stable fixed point and away from the unstable one.

growth phase prior to reentering the cell cycle. The start is the point at which the cell is committed to another round of division and is marked morphologically by the first appearance of a bud. DNA replication also begins at this time. The chromosomes organize on the spindle and then separate in mitosis. The new daughter can then detach from the mother. The cell cycle is coordinated by the cyclin genes [2], and some of the genes that figure in the following discussion are shown in Fig. 2(b). The network is conveniently decomposed into two oscillators [12]. The negative feedback oscillator is most prominent in rapidly cycling systems such as fly embryos and entails an alternation between DNA replication and mitosis. The level of the mitotic cyclin Clb2 builds up following the start. It must be degraded for mitotic exit and this is accomplished by its negative regulator, a complex involving Cdc20, that is activated by Clb2 itself. The relaxational oscillator is built around two fixed points, a low Clb2 growth phase, G1 (enforced by two Clb2 repressors, Cdh1, and Sic1), followed by a high Clb2 phase encompassing start and mitosis. The G1 phase terminates when a second set of cyclins Cln1,2,3 reach a level sufficient to repress the repressors of Clb2 and initiate start. Similarly the high Clb2 state is destabilized in part when a gene, CDC14, is activated which reverses the phosphorylations targeted by Clb2. Relaxational oscillators exhibit metastability and hysterisis.

With a view towards future experiments, we will investigate the mode-locking properties of the model of Refs. 6, 12, and 13. The mass in this model is the surrogate for all growth processes. It is unique among all the variables in that its growth is exponential at a rate defined by the parameter μ and uncoupled from the others. Then, in accordance with a well-established genetic pathway (in which not all the molecular components are known [15]), the mass controls the activation rate for genes (mainly CLN3) that control Start and terminate G1 (Fig. 2). Budding yeast divide asymmetri-

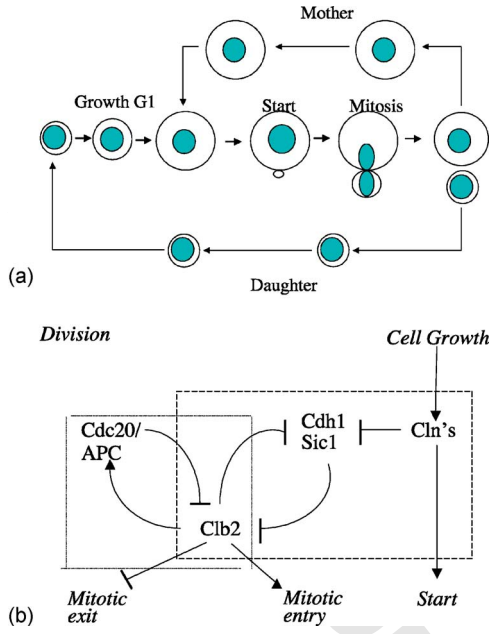

FIG. 2. (Color online) Schematic of the cell cycle in budding yeast (a). There is a variable length period of growth until the cell reaches a size sufficient for "Start," when the cell commits to a new round of division. The bud that will become the new cell first appears at "Start" and DNA replication begins. When cell division occurs the mother is generally larger than the daughter and reenters the cell cycle sooner. The principal proteins controlling the cell cycle are shown in (b) with some of the couplings to the events in (a) shown in *italic*. The proteins comprising the relaxational oscillator are in the dashed box and organized around two fixed points defined by the mutual inhibition of Clb2 and Cdh1+Sic1. In the negative feedback oscillator (dotted box), Clb2 activates its repressor, the Cdc20-APC complex (see text).

cally, the daughter is smaller at separation and takes longer to divide again. To fit the cycle times of mother and daughter, Chen *et al.* [6] introduce an *ad hoc* parameter, the mother-daughter mass ratio at division, This parameter, together with μ then fit the periods of mother and daughter. This system cannot mode lock since the periods are defined by numerical parameters in the model and cannot vary in response to an external forcing.

We therefore adapt another model of growth. The total mass still grows exponentially at a rate μ, but we now impose that once the bud forms, all the new mass generated goes into the daughter. As a consequence, the mother grows larger with each successive birth (i.e., it accrues all mass created prior to budding in G1), and the mechanics of cell growth then dictate that its period decreases with each birth. It cannot lock. The mass of the daughter, however, is now coupled with the other variables of the system so mode locking is a possibility. This model was also considered in Ref. [6] and accords with the observation that the size of the mothers viewed in the microscope is increasing. They rejected it because the periods of mothers and daughters did not match published experiments [16]. There may be other ways to fix this problem, and we focus on the daughter cells with this mass partition formula for the remainder of this paper. To better match experiments, we change μ from 0.005776 to 0.008 giving a daughter cycle time of 138 min (with the time from bud to division of 50 min) and a cycle time of 68 min for first time mothers, which decreases by 3 min with each birth. All other parameters are taken from Ref. [6].

TABLE I. The period intervals for mode locking for various variables and strengths of perturbation. The perturbation is a square pulse (duration period/6 for Cln2,3 and period/20 for Clb2) added to the variable. The units are only defined in relation to the model, but the ratios are meaningful. To give a sense of scale in more physical terms, the ratio of the maximum amplitude of the forced variable, to its wt value, is given in parenthesis. The amplitude ratio with and without forcing varies considerably with the phase of the force, and is least ambiguous for a large amplitude pulse, so we only include it for the first entry for each variable.

Variable	Pulse amplitude (ratio with wt)	Period interval (min)
Cln3	0.004 (2)	100–138
	0.002	114–138
	0.001	128–138
Cln2	0.1 (2.2)	108–138
	0.03	95–138
	0.01	125–138
Clb2	0.001 (<1.1)	139–149

Even though the model differs quantitatively from experiment as to cycle periods, we believe it still can make informative predictions about how effective the coupling to various genes will be for controlling the cycle time. Observation of locking *per se* would not be a direct test of our mass partitioning model since our geometric discussion implies that unless locking is explicitly prohibited by the equations, it will occur. The question is rather how prominent are the mode-locked regions in parameter space.

To achieve locking, the most obvious variables to externally couple to are those that directly sense the mass. Both, in experiment and the model, a small mass at birth leads to a longer cycle time and a larger mass on the next division, and thus, mass homeostasis [15]. In conformity with experiments, the model uses the mass to achieve homeostasis primarily via terms in the equations for the cyclins Cln2 and Cln3 whose growth controls the duration of G1.

It is experimentally feasible to augment the production of a desired gene product by placing it under the control of regulatory DNA that responds to the presence of a metabolite such as galactose. Then, pulsing a metabolite into the solution induces expression of the gene. To be modestly faithful to what might be done, we model the external perturbation as a square pulse added to the production rate from the gene of interest (the active forms of the protein sometimes require additional transformations and they cannot be coupled to directly). A summary of the genes and parameter ranges we explored is provided in Table I.

Figure 3 conveys a global impression of how the mass of daughter cells evolves through several cycles, as T is varied through the regime of locking. A convenient reporter for the cell cycle is the daughter mass, which becomes nonzero at

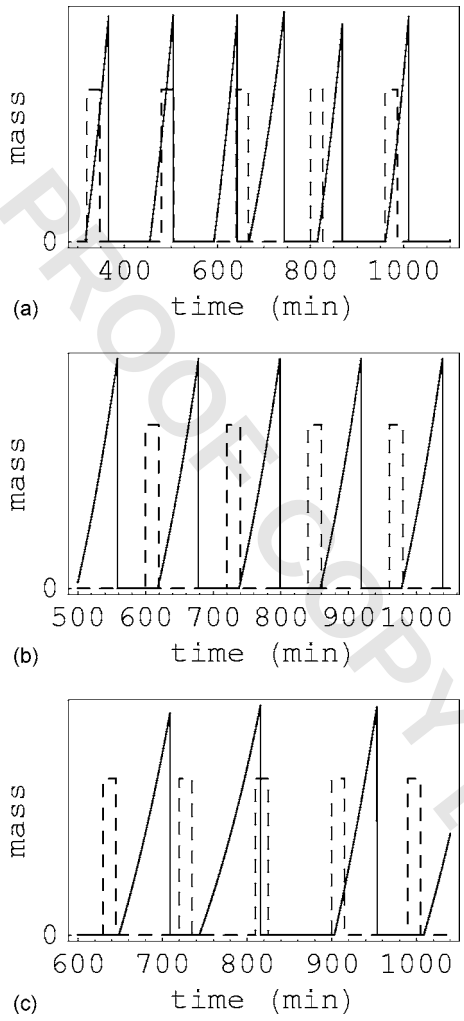

FIG. 3. The daughter mass (solid line, arbitrary units) as a function of time for impulses of Cln3 (dashed) with periods T, longer than the locking interval [T=160 min, (a)], within the mode-locked interval [T=120 min, (b)], and shorter than the mode-locked interval [T=90 min, (c)]. The amplitude of the perturbation is given by the first entry in Table I. Note that there is an extra cell cycle in (a) and an extra pulse in (c). The natural period of the cell is 138 min, which is the average period in (c).

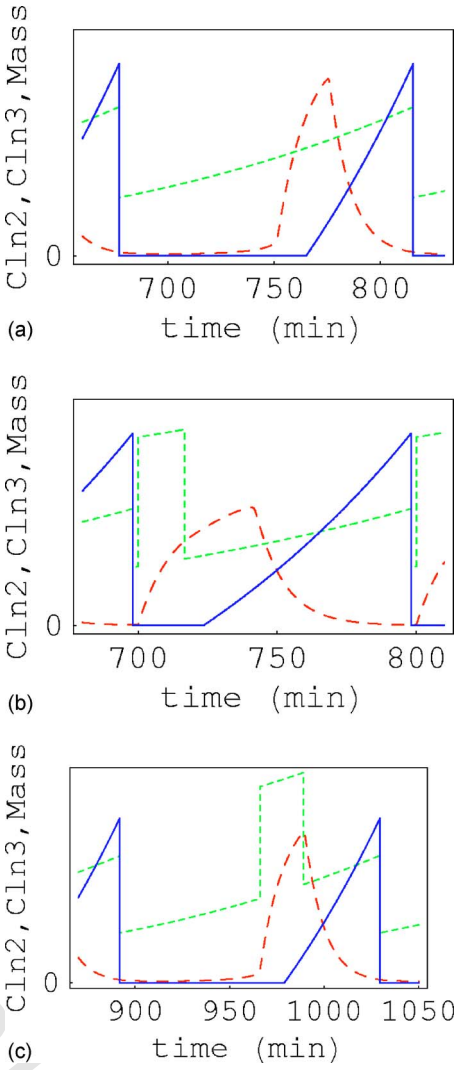

FIG. 4. (Color online) Time traces of the principal variables controlling G1, Cln2 (red, long dash), Cln3 (green, short dash), and the daughter mass (blue, solid) for wt cells period 138 (min) in (a), and cells mode locked to pulses in Cln3 (amplitude 0.004) with period 100 (min) in (b) and 138 (min) in (c). The units on the y axis are arbitrary. The external pulse to Cln3 is clearly visible in its traces. The daughter mass increases from zero when the bud initiates. It is reset to zero at division.

bud time, and resets to zero at division. When T is too long, the cell will occasionally add an extra cycle between pulses, and when T is too short, extra pulses are inserted between cell division cycles. The mode-locked solution has fixed relative phase between the perturbation and the cell variables. In terms of the Poincaré map Eq. (2), when T is too long, n iterations of the map will give a total phase change of $2\pi(n+1)$, and when T is too short there will be relative phase loss. Mode locking corresponds to a stable fixed point. We now consider in more detail the relation among the physical variables when locking occurs and it is sufficient to just plot one period of the orbit.

The effects of perturbing the G1 cyclins are illustrated in Figs. 4(a)–4(c) for Cln3. The dominant pathway is Cln3 activates Cln2, and both then induce budding. The shortest period possible occurs when the pulse comes just after division (at the beginning of G1). It then triggers the premature activation of Cln2, which in turn results in early budding and a shortened G1. The time from bud to division is longer than wt (75 vs 50 min) and the mass at budding about the same. The increased time following budding is needed to maintain the daughter mass. The longest period for which locking is possible is just the wt period, Fig. 4(c), when the pulse of Cln3 falls at the time Cln2 normally activates. The time from bud to division is also equal to the wt value, but the mass is 15% smaller. When the external period is longer than wt, normal activation of budding still occurs, and the relative phase of pulse and division evolves in time. By augmenting Cln3 (or Cln2) one can only shorten the period, not lengthen it. Even when the external period is 138 (i.e., wt), phase locking is evident by the stable phase relation between the onset of the pulse and the onset of Cln2. For Cln3, the mode-

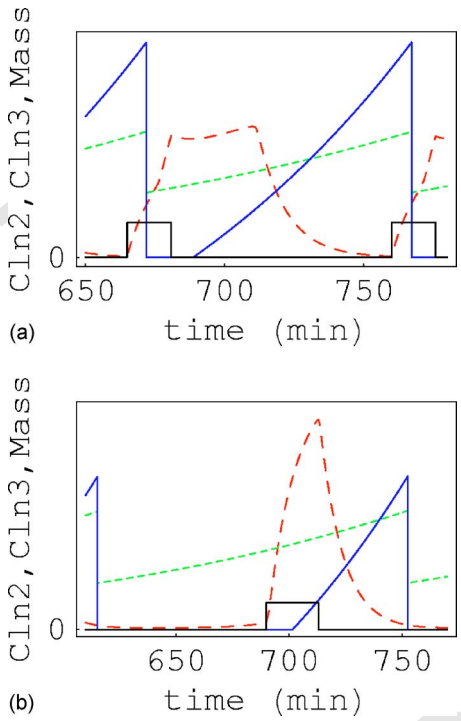

FIG. 5. (Color online) The same variables as in Fig. 4, but with the external square pulse (solid black line) applied to the differential equation of Cln2. The pulse amplitude corresponds to the second Cln2 entry in Table I, and the limiting mode-lock periods 95 min (a) and 138 min (b) are shown. [Note that the amplitude of Cln2 in (b) is different from wt in Fig. 4(a).]

locked interval scales as a linear function of f, Table I.

Perturbing Cln2 gives similar effects, Fig. 5. The shortest period is achieved with a very attenuated G1 (coupled to an augmented time of bud-division of 79 min), and a Cln2 profile that is actually lower than wt but broader. [In contrast to Cln3, which is an instantaneous function of the mass in the model, here we added the pulse to d Cln2/dt, so its square shape is not so visible in Cln2(t).] For the longest locking period, Fig. 5(b), the shape of the Cln2 trace is similar to wt, but the amplitude is 25% greater. The external pulse is phased with the natural onset of Cln2(t). The largest amplitude pulse in Table I for Cln2 is clearly in the nonlinear regime, since the range of mode-locked periods is larger when the amplitude decreases.

The G1 cyclins, driven by the mass, are the "slow" variables which move the system along one of the stable branches of the relaxation oscillator, in the terminology of [4,13]. During this period the mitotic cyclin Clb2 is strongly repressed (i.e., Clb2=0 is a stable solution). This repression disappears at budding and Clb2 grows until it induces its inhibitor Cdc20, which eventually leads to the destruction of Clb2, cell division, and the next G1. The interplay of these two proteins constitutes the negative feedback oscillator [13], and it is natural to ask whether these can be mode locked.

The answer is complex, as suggested in Fig. 6. Cdc20 only represses when it is activated. Its activated form is strongly suppressed until the spindle forms, encoded in the model by when the variable *spn* hits 1. When this happens,

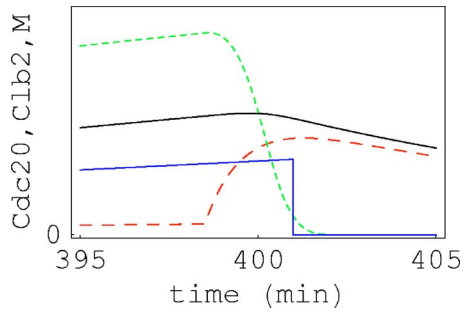

FIG. 6. (Color online) The events in the short interval surrounding division showing active Cdc20 (red, long dash), Clb2 (green, short dash), daughter mass (blue, solid step down), and total Cdc20 protein (black, solid curve). The spindle forms (spn=1) when the red curve begins to increase. The curves for the mode-locked and wt variables are indistinguishable.

there is already a substantial pool of total protein (represented by the variable Cdc20T), which without significant change rapidly converts to active form, destroys Clb2, and triggers mitosis. The time between spn=1 and division is 2.5 min, i.e., very short compared with the cycle time. Hence, when we perturb Cdc20T (which is the only variable physically accessible), the first appearance of active Cdc20 is unchanged, since that is controlled by *spn*, and even the decay of Clb2 is minimally affected, since much less than the maximum available Cdc20T suffices, when active, to eliminate Clb2. Although the regulatory linkage provided by Cdc20 is definitely needed to inhibit Clb2, its dynamics do not play a role in the model.

A standard method for synchronizing yeast cells is to turn off the production of Cdc20, which arrests all cells in mitosis [17]. (When it is restored, the population of cells dephases after about 1.5 division cycles due to the natural variability between mother and daughter periods.) If we eliminated all endogenous sources of Cdc20T, in particular the induction by Clb2, we could not mode lock the system with pulses of Cdc20T. For some parameters, the suppression of Clb2 was not strong enough, the mass increased from division to divisions and ultimately the model is no longer believable. Other parameters gave persistent oscillations, but either with multiple periods or a superperiod imposed on the cell cycle. There is probably a curve in the amplitude-period plane (f,T) where the division cycle follows the perturbation, but not a region, which is indicative of mode locking. The failure to mode lock in this case does not contravene our geometric arguments, since with no endogenous source of Cdc20 there is no periodic orbit when f=0. Our entire construction is predicated on a small external perturbation to a periodic system.

Locking in a restricted parameter range is possible by pulsing in Clb2, Table I. *spn* grows in response to the level of Clb2. So, by adding Clb2 just after budding, *spn* reaches 1 a bit sooner, division occurs earlier (time bud to division is 45 min, shorter than wt), mass at division is reduced, and the overall daughter period is then lengthened. For the minimal locking period, which approximates wt, the Clb2 pulse is phased just to terminate with budding, so it is largely destroyed by the repression of Clb2 that occurs prior to bud-

ding. (Technically we only perturb the variable Clb2T, but its stoichiometric inhibitor, Sic1, is off until G1, so active Clb2 is the same as the total.) Substantially larger perturbations administered to Clb2 mode lock over a smaller range of periods for reasons we do not understand. If the model captures how a cell exits mitosis, then we doubt perturbing Clb2 or Cdc20 is a viable option for mode locking.

DISCUSSION

What are the prospects for actually mode-locking real cells? The uncertainties in the model we solved, in particular the mass partitioning assumption, should not be impediments in principle since mode locking is a generic property of nonlinear systems. Much more crucial was the assumption that the model is deterministic, since real cells are quite variable for reasons that are not understood. Cellular variability could either be due to molecular noise (small numbers of molecules), a variable environment, or deterministic chaos. If the noise is extrinsic to the equations, the Poincaré map is still a useful guide to the dynamics. In the simplest case there will be one stable and one unstable fixed point. The relative phase between the perturbation and the cycle of a particular cell depends on when the cell is born. For some phases it will be pushed away from the unstable point, gain or lose a cycle, and then be captured by the stable fixed point, Fig. 1. Noise will either just agitate the phase in the vicinity of the stable solution, or if larger (or the stable domain is small because the system is approaching the limits of mode locking), cause excursions into the vicinity of the unstable point that move once around the circle to be recaptured by the stable point

The same considerations govern the behavior of a field of cells. Assume we start with a single cell and watch it grow into a cluster. Even in the absence of noise, the preceding calculation only guarantees the locking of a single cell, since we followed the dynamics from daughter to daughter. The founding mother will produce multiple daughters but these will be born out of phase with the first daughter (and her first daughters, etc.). But any chain of primary daughters will get pulled into the same fixed point. At this stage the experimenter might wish he were studying fission yeast, which divide symmetrically. (Assuming again that the period is not a fixed number but determined by coupling among the other variables in the oscillator.)

The calculations described here were carried out with a modified version of an early cell cycle model [6]. Recently this model was updated [7] to include new machinery, including explicit checkpoint mechanisms and the mitotic exit network controlling the Cdc14 phosphates [18]. It will be interesting to see if this model will allow extension of the mode-locking analysis. For example, we interpreted our inability to mode lock with Cdc20 as being due to checkpoint inactivation of Cdc20 activity. In the new model, it would be possible to test for mode locking in the absence of the checkpoint machinery. In addition, we have experimentally interpreted Cdc14 inactivation as similar to preventing establishment of the low-Cdk state in the relational oscillator branch of the budding yeast cell cycle [13]. Trying to mode lock with Cdc14 could thus be the complementary situation to mode locking with Cln3, which acts on the bistable state in the opposite direction.

ACKNOWLEDGMENTS

E.D.S. was supported by the NSF under Grant No. DMR0129848, and F.R.C. by PHS GM47238.

[1] K. Nasmyth, Cell **107**, 689 (2001).
[2] A. Murray and T. Hunt, *The Cell Cycle, An Introduction* (Oxford University Press, New York, 1993).
[3] P. T. Spellman, G. Sherlock, M. Q. Zhang, V. R. Iyer, K. Anders, M. B. Eisen, P. O. Brown, D. Botstein, and B. Futcher, Mol. Biol. Cell **9**, 3273 (1998).
[4] B. Novak, A. Csikasz-Nagy, B. Gyorffy, K. Nasmyth, and J. J. Tyson, Philos. Trans. R. Soc. London, Ser. B **353**, 2063 (1998).
[5] A. Sveiczer, A. Csikasz-Nagy, B. Gyorffy, J. J. Tyson, and B. Novak, Proc. Natl. Acad. Sci. U.S.A. **97**, 7865 (2000).
[6] K. C. Chen, A. Csikasz-Nagy, B. Gyorffy, J. Val, B. Novak, and J. J. Tyson, Mol. Biol. Cell **11**, 369 (2000).
[7] K. C. Chen, L. Calzone, A. Csikasz-Nagy, F. R. Cross, B. Novak, and J. J. Tyson, Mol. Biol. Cell **15**, 3841 (2004).
[8] J. Guckenheimer and P. Holmes, *Nonlinear Oscillations, Dynamical Systems, and Bifurcations of Vector Fields* (Springer-Verlag, Berlin, 1983).
[9] D. Battogtokh and J. J. Tyson, Chaos **14**, 653 (2004).
[10] J. R. Pomerening, E. D. Sontag, and J. E. Ferrell, Jr., Nat. Cell Biol. **5**, 346 (2003).
[11] W. Sha, J. Moore, K. Chen, A. D. Lassaletta, C. S. Yi, J. J. Tyson, and J. C. Sible, Proc. Natl. Acad. Sci. U.S.A. **100**, 975 (2003).
[12] F. R. Cross, V. Archambault, M. Miller, and M. Klovstad, Mol. Biol. Cell **13**, 52 (2002).
[13] F. R. Cross, Dev. Cell **4**, 741 (2003).
[14] F. Li, T. Long, Y. Lu, Q. Ouyang, and C. Tang, Proc. Natl. Acad. Sci. U.S.A. **101**, 4781 (2004).
[15] M. N. Hall, M. Raff, and G. Thomas, *Cell Growth* (Cold Spring Harbor Lab Press, New York, 2004).
[16] P. G. Lord and A. E. Wheals, J. Cell. Sci. **50**, 361 (1981).
[17] M. Shirayama, A. Toth, M. Galova, and K. Nasmyth, Nature (London) **402**, 203 (1999).
[18] D. D'Amours and A. Amon, Genes Dev. **18**, 2581 (2004).